Transport Analysis of High-Z Impurities Including Sawtooth Effects in a Tokamak System

Ikuhiro YAMADA, Kozo YAMAZAKI, Tetsutarou OISHI, Hideki ARIMOTO and Tatsuo SHOJI

Nagoya University, Nagoya, Aichi 464-8603, Japan

(Received 14 January 2009 / Accepted 27 September 2009)

In fusion reactors, high-Z materials will be used to balance the need to accommodate high heat load on divertor plates against consistency between fusion burning plasmas and plasma facing component (PFC) materials. However, high-Z impurities from these PFCs cause large radiation loss even if the amount of impurities is quite small. High-Z impurity transport analysis including sawtooth effects is carried out using the toroidal transport analysis linkage (TOTAL) code. The Bohm-type anomalous transport model for the core plasma and the anomalous inward flow model for impurity ions are used in addition to neoclassical transport. After comparisons with Joint European Torus (JET) impurity transport data, sawtooth effects on impurity transport in ITER are clarified with a simplified full magnetic reconnection model. The critical levels of impurity concentration in ITER are found to be 4.0 % for carbon, 0.1 % for iron, and 0.008 % for tungsten with respect to electron density. Forming an internal transport barrier (ITB) for electron density can prevent high-Z impurity accumulation. Also, sawtooth oscillation is shown to be beneficial, reducing radiation loss from the plasma core by about 20 %, although it might lead to unfavorable fusion power fluctuation of 10 %.

Keywords: impurity, transport, sawtooth oscillation, internal transport barrier, tokamak

DOI: 10.1585/pfr.5.S1022

1. Introduction

In fusion reactors, the divertor plate and other plasma facing component (PFC) materials interact with hot plasma by ion backscattering and chemical and physical sputtering processes, and then yield impurities into the plasma. In particular, heat loads on divertor plates are predicted to be very large, and high-Z materials such as tungsten will be used for such parts due to their high heat conductivity and low erosion rate. However, the resulting high-Z impurity ions tend to accumulate in the plasma core due to strong inwardly directed drift velocities caused by neo-classical convection, causing large impurity radiation loss. Furthermore, they displace reacting ions by the large number of electrons they release, diluting the fuel.

The radial distribution of impurity ions in a tokamak is calculated by using a 1.5-dimensional (1.5-D) transport code toroidal transport analysis linkage (TOTAL) [1]. In Section 2, the simulation code used in this paper is described. In Section 3, typical machine parameters and plasma parameters are given. In Section 4, simulation results are presented. First, we clarify the permissible impurity level for the ITER plasma. Second, we show the impurity behavior in plasmas with an internal transport barrier (ITB). Third, the effects of sawtooth oscillation on impurities are described. In Section 5, a summary and conclusion are presented.

author's e-mail: i-yamada@ees.nagoya-u.ac.jp

2. Numerical Model

2.1 Transport Model

To investigate transport of fuel and impurity ions in a tokamak, we used a 1.5-D (1-D transport/2-D equilibrium for tokamak) time-dependent simulation model with low-Z gas and high-Z metal impurity dynamics. The plasma density n_e, n_i and temperature T_e, T_i are described as follows.

$$\frac{\partial n_e}{\partial t} + \frac{1}{V'}\frac{\partial}{\partial \rho}V'\Gamma_e = S_P \tag{1}$$

$$\sum_i z_i n_i \approx n_e \tag{2}$$

$$\frac{3}{2}\frac{\partial n_e T_e}{\partial t} + \frac{1}{V'}\frac{\partial}{\partial \rho}\left\{V'\left(q_e + \frac{5}{2}\Gamma_e T_e\right)\right\} = P_{He} - P_{ei} - P_{rad} - \Gamma_e E_r \tag{3}$$

$$\frac{3}{2}\frac{\partial n_i T_i}{\partial t} + \frac{1}{V'}\frac{\partial}{\partial \rho}\left\{V'\left(q_i + \frac{5}{2}\Gamma_i T_i\right)\right\} = P_{Hi} - P_{ei} - P_{cx} - z_i\Gamma_i E_r \tag{4}$$

Here, ρ is the normalized radius, and V is the volume defined by the equilibrium magnetic surface. The radiation loss P_{rad} is the sum of bremsstrahlung radiation, impurity line radiation, and synchrotron radiation powers.

For the anomalous part of the transport coefficients, the Bohm-type model based on Joint European Torus (JET) experimental data [2] is used in this paper,

$$\chi_e = \chi_i = \alpha_B \frac{T_e}{B_t} q_\Psi^2 / L_{Pe}^*, \tag{5}$$

where, T_e, B_t, and q_Ψ are the electron temperature (eV), toroidal magnetic field (T), and magnetohydrodynamic (MHD) safety factor. L^*_{Pe} is the scale length of the pressure gradient normalized by the minor radius. The coefficient α_B used here is 3.3×10^{-4} using SI units and eV.

2.2 Impurity Model

We examined high-Z impurities with a model for impurities in TOTAL; the multi-species dynamic impurity code IMPDYN [3] was used to model the ionization states, and the NCLASS code [4] was used for the full neoclassical transport of each charge state considering arbitrary aspect ratio and collisionality.

For the impurity dynamics [5, 6], the rate equation and diffusion equation are solved using the IMPDYN code [3] coupled with the ADPAK atomic physics package [7], which can calculate the cooling rate,

$$\frac{\partial n_k}{\partial t} = -\frac{1}{V'}\frac{\partial}{\partial \rho}(V'\Gamma_k) + [\gamma_{k-1}n_{k-1} + \alpha_{k+1}n_{k+1} - (\gamma_k + \alpha_k)n_k]\,n_e + S, \tag{6}$$

$$\Gamma_k = \Gamma_k^{\mathrm{NCs}} + \Gamma_k^{\mathrm{NCa}} - D_k(\rho)\frac{\partial n_k}{\partial \rho} + V_k(\rho)\,n_k \tag{7}$$

with ionization rate γ_k, recombination rate α_k, and particle source term S_k. Here, a constant anomalous diffusion coefficient D_k and simply modeled inward velocity $V_k = V(a)(r/a)$ are used for impurity anomalous transport ($V_k < 0$ corresponds to inward velocity). The main fuel neutrals are calculated by the AURORA Monte Carlo code [8].

The neoclassical impurity flux in a tokamak is expressed by

$$\Gamma_k^{\mathrm{NCs}} = -D_k^{\mathrm{NC}}\nabla n_k + D_k^{\mathrm{NC}} n_k \left[\sum_{l\neq k}(g_{nl\to k}\nabla n_l/n_l) + g_{\mathrm{Ti}}\nabla T_i/T_i + g_{\mathrm{Te}}\nabla T_e/T_e\right]. \tag{8}$$

In the simulation, the impurity source was defined as the impurity neutral flux on the plasma boundary. The neutral impurity density profile $n_0(\rho)$ is assumed to be

$$n_0(\rho) = -\frac{V'(1)\Gamma_0(1)}{V'(\rho)v_0}\exp\left(-\frac{1}{v_0}\int_1^{\rho} d\rho n_e(\rho)\gamma_0(\rho)\right), \tag{9}$$

derived from

$$\frac{\partial n_0}{\partial t} = -\frac{1}{V'}\frac{\partial}{\partial \rho}(V'\Gamma_0) - \gamma_0 n_e n_0 \approx 0\,, \tag{10}$$

$$\Gamma_0(\rho) \approx -n_0(\rho)v_0\,. \tag{11}$$

Here, $\Gamma_0(1)$ is the neutral impurity flux at the plasma boundary ($\rho = 1$), and v_0 is the neutral impurity inward velocity (assuming an energy of 10 eV). The symbols γ_0 and n_e are the ionization coefficient and electron density near the plasma boundary, respectively.

To clarify the effect of impurity ions, steady-state burning plasma conditions were established without impurities. Then, a continuous neutral impurity influx was introduced, and after a transient phase, the system settled into a new radiation-enhanced steady state.

Table 1 Typical machine and plasma parameters.

	ITER	JET
R[m]	6.2	2.9
a[m]	2	0.95
κ	1.7	1.6
δ	0.3	0.2
B[T]	5.3	3.45
Ip[MA]	15	4

3. Model of Tokamak and Helical Plasmas

To simulate impurity ion behavior, we considered reacting or burning plasmas in JET and ITER. Typical plasma parameters of these machines are shown in Table 1.

4. Simulation Results

4.1 Permissible Impurity Level

We clarify the critical impurity content for a tokamak plasma with respect to electron density to maintain $Q > 10$. Here, ITB plasma operations with a $\rho = 0.6$ foot-point are assumed. To create the ITB, we assume the following simplified transport model, which reduces the diffusion coefficient and thermal diffusivity near $s \sim 0$.

$$\chi_e = \chi_i = \chi_0\left(1 + \rho^2\right)E(s) \tag{12}$$

$$E(s) = \{1 + \exp[c(s+1)]\}^{-1} + \{1 + \exp[-c(s-1)]\}^{-1} \tag{13}$$

Here, s is the shear parameter, and c is adjusted so that the transport reduction coefficient $E(s)$ is reduced to 1/10 at $s = 0$. In this paper, the parameter s is replaced by $20(r - r_{\mathrm{ITB}})/a$ to produce an ITB artificially. In ITER, the critical concentrations of impurities that reduce the Q value from 15 to 10 are 4.0 % for carbon, 0.1 % for iron, and 0.008 % for tungsten, as shown in Fig. 1.

4.2 Effects of Steep Density/Temperature Gradient

To control the impurity influx, modifying the edge plasma density profile might be beneficial. According to the neoclassical theory, a finite gradient of temperature (i.e., negative $\nabla T/T$) might contribute to the impurity shielding effect, but a finite density gradient leads to the impurity pinching effect. We investigated ITB effects on impurities near the plasma edge, because impurities mainly affect that region. In this analysis, we demonstrate the profiles of plasma parameters for the reference ITER inductive scenario based on the ELMy H-mode regime with fusion power P_{fus} = 400 MW, Q value > 10, toroidal magnetic field B_0 = 5.3 T, plasma current I_P = 15 MA, and RF heating power P_{RF} = 40 MW. Figure 2 shows the effects of the edge electron density profile in the case of an ITB footpoint at $\rho = 0.8$. When the edge density profile is assumed to be rather flat near the temperature ITB, the impurity line radiation as well as impurity density can be reduced, as shown in the figure. This result indicates that ITB formation, e.g., by pellet injection, can prevent high-Z impurities from accumulating near the edge region.

4.3 Effects of Sawtooth Oscillation

Sawtooth oscillations are periodic, MHD-initiated mixing events that occur in a tokamak plasma when the central safety factor is less than unity. In this analysis, a sawtooth threshold value $q(0) = 0.85$ is assumed. Sawtooth oscillation is known to affect the transport of the main plasma and impurities by flattening the radial profile of densities and temperatures periodically in the core plasma. Thus, if inward anomalous convection is present, small sawtooth oscillation may be considered beneficial in preventing the accumulation of impurities in the core region. In this paper, we simulate argon seeding experiments in JET [9, 10] and also predict the impurity (Ar/W) behavior in ITER discharge with sawtooth oscillation in the case of an existing relatively large inward drift velocity for impurities.

A simplified sawtooth model included in the TOTAL code evolves the plasma profiles within a crash. In the model, when the central safety factor $q(0)$ is less than

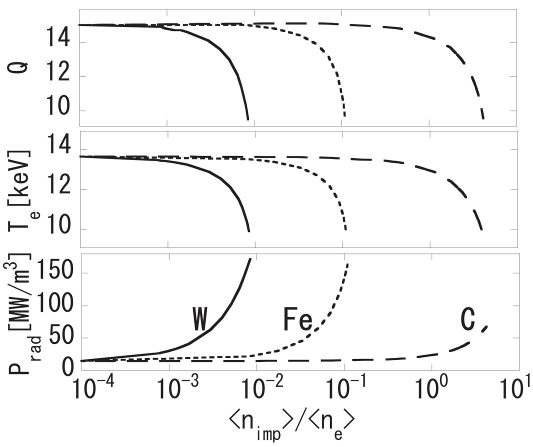

Fig. 1 Plasma parameter variation versus impurity concentration.

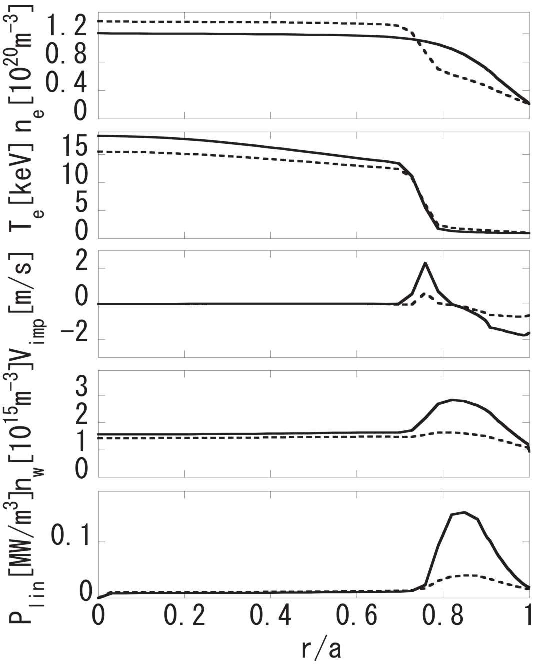

Fig. 2 Effects of edge density profile on impurity transport in ITER ITB plasma. Solid line corresponds to the density profile with no ITB gradient, and dashed line corresponds to the ITB density profile.

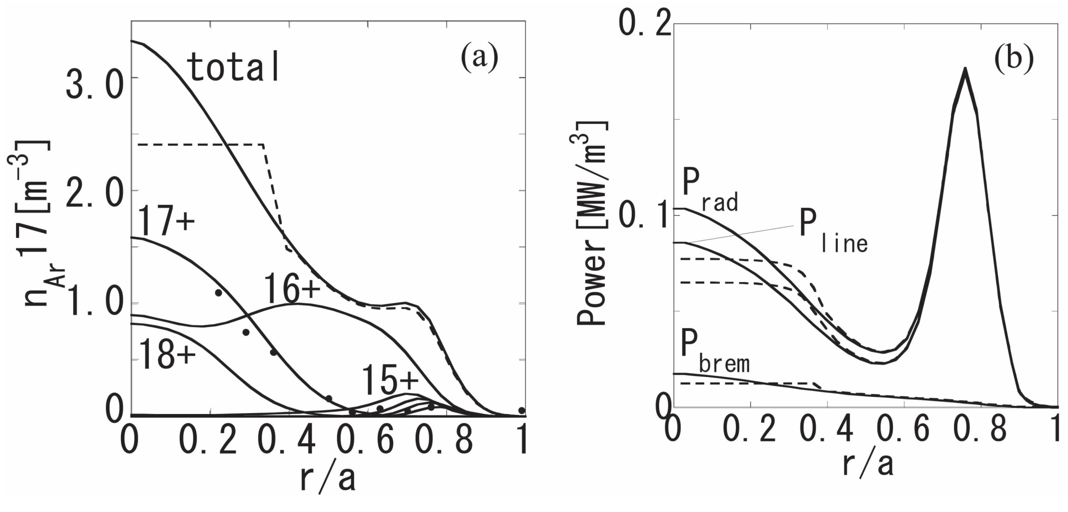

Fig. 3 Simulated sawtooth oscillation effect on argon impurities in JET plasma. Figures (a) and (b) show the total impurity density profile and total radiation profile, respectively, before (solid line) and after (dashed line) sawtooth crash. Points (•) show the JET experimental Ar^{18+} ion density [9].

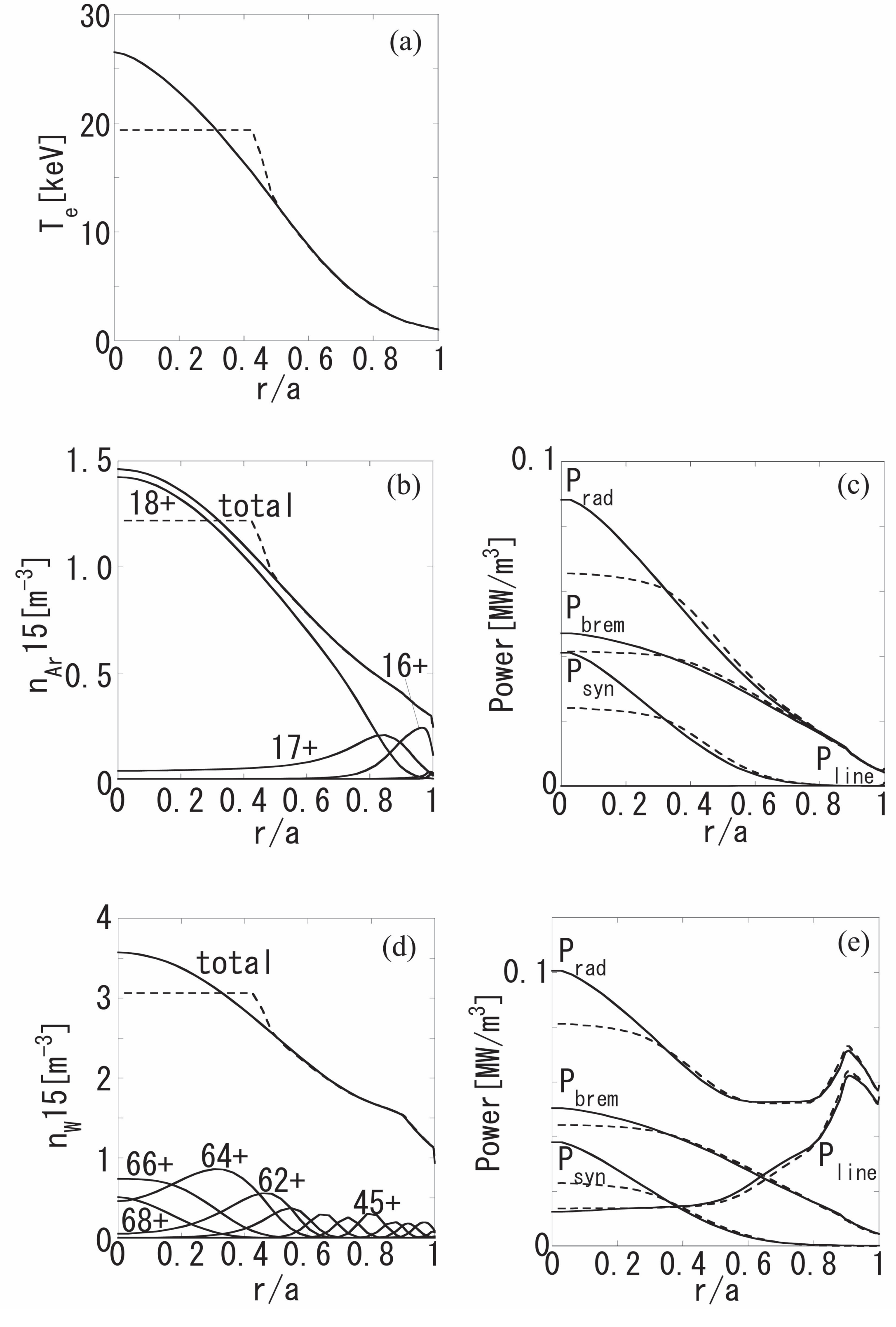

Fig. 4 Simulated sawtooth oscillation effects on impurity ions in ITER plasma. Figure (a) shows the radial profile of electron temperature. Figures (b) and (c) show the total impurity density profile and total radiation profile $P_{\rm rad}$, respectively, in the case of argon, before (solid line) and after (dashed line) sawtooth crash. Radial profiles of line radiation $P_{\rm line}$, bremsstrahlung radiation $P_{\rm brem}$, and synchrotron radiation $P_{\rm syn}$ are also shown in Figure (c). Figures (d) and (e) show the corresponding results for tungsten impurities.

a threshold value, the pressure and current profiles are quickly changed to be flat inside the inversion radius, based on Kadomtsev's full magnetic reconnection model.

As a result, in JET experiments, sawtooth oscillation is found to be effective for controlling impurities [9, 10]. Figure 3 shows that simulated sawtooth oscillation in JET can prevent impurities from accumulating in the plasma core and can reduce corresponding impurity line radiation by about 25 % and total radiation loss from the plasma core by about 26 %. These results roughly agree with experimental data.

On the other hand, in ITER, as shown in Fig. 4, since argon impurities are almost fully ionized, the corresponding line radiation is nearly zero along the whole radius except at the plasma boundary. Similarly, in the case of tungsten impurities, the existence of highly charged ions in the core region makes the line radiation profile hollow. In both cases, sawtooth oscillations reduce bremsstrahlung radiation and synchrotron radiation from the plasma core, and a reduction in radiation loss from the plasma center of about 20 % might be realized, as shown in Fig. 4, although the line radiation profile is not affected. This demonstrates that sawtooth activities can effectively reduce radiation loss from the plasma core, which is caused by a temperature and density drop due to internal disruption, and might cause the fusion power to fluctuate by about 10 %.

5. Summary and Conclusion

We investigated the transport of high-Z impurity ions, including sawtooth effects, and show the following results:

(1) In ITER, the critical levels of impurity concentration that reduce the Q value from 15 to 10 are 4.0 % for carbon, 0.1 % for iron, and 0.008 % for tungsten with respect to electron density.

(2) ITB formation with respect to electron density, such as that induced by pellet injection, can prevent high-Z impurity ions from accumulating near the edge region.

(3) Sawtooth oscillation is beneficial for reducing radiation loss from the plasma core by about 20 %, although it leads to unfavorable fusion power fluctuation of 10 %.

[1] K. Yamazaki and T. Amano, Nucl. Fusion **32**, 633 (1992).

[2] A. Taroni *et al.*, Plasma Phys. Control. Fusion **36**, 1629 (1994).

[3] T. Amano, J. Mizuno and J. Kako, ‘Simulation of Impurity Transport in Tokamak’, Internal report IPPJ-616, Institute of Plasma Physics, Nagoya Univ. (1982).

[4] W. A. Houlberg *et al.*, Phys. Plasmas **4**, 3230 (1997).

[5] Y. Murakami, T. Amano *et al.*, J. Nucl. Mater. **313-316**, 1161 (2003)

[6] K. Yamazaki *et al.*, J. Plasma Fusion Res. SERIES **7**, 102 (2006).

[7] R. A. Hulse, Nucl. Technol. Fusion **3**, 259 (1983).

[8] M. H. Huges and D. E. Post, J. Comput Phys. **28**, 43 (1978).

[9] M. E. Puiatti *et al.*, Plasma Phys. Control. Fusion **44**, 1863 (2002).

[10] M. E. Puiatti *et al.*, Plasma Phys. Control. Fusion **45**, 2011 (2003).